JOURNAL OF AGRICULTURAL AND FOOD CHEMISTRY
ARTICLE

J. Agric. Food Chem. 2010, 58, 2253–2259 2253
DOI:10.1021/jf903731s

Hydrolysis Behavior of Bamboo Fiber in Formic Acid Reaction System

YONG SUN AND LU LIN*

State Key Laboratory of Pulp and Paper Engineering, South China University of Technology, Guangzhou, 510641, P. R. China

The process of conversion of bamboo fiber into fermentable glucose in the formic acid reaction system was investigated using cross-polarization/magic angle spinning ^{13}C-nuclear magnetic resonance (CP/MAS ^{13}C NMR), X-ray diffraction. The results indicated that formic acid as an active agent was able to effectively penetrate into the interior space of the cellulose molecules, thus collapsing the rigid crystalline structure and allowing hydrolysis to occur easily in the amorphous zone as well as in the crystalline zone. The bamboo fiber was hydrolyzed using formic acid and 4% hydrochloric acid under mild conditions. The effects of temperature (55−75 °C), retention time (0−9 h) and catalyst, the concentration of glucose and the degradation pathway of glucose were analyzed. The main degradation pathway of glucose is that the hydroxyl group on the 2-carbon is protonated and cleaved off. Aluminum iso-propoxide prevented the degradation of glucose, and the acetone promoted the degradation of glucose to levulinic acid.

KEYWORDS: Bamboo fiber; CP-MAS ^{13}C NMR; X-ray; hydrolysis; pathway; degradation; formic acid

INTRODUCTION

The unbalanced distribution of global petroleum resources and considerable price fluctuation are forcing the chemical industry to find alternative raw materials for the production of basic chemicals. On the other hand, agriculture produces an abundant amount of renewable commodities, such as cereals grains, oil seeds and agricultural biomass wastes each year. The lack of demand for agricultural commodities has caused their prices to fall. The agricultural biomass wastes usually are discarded. The combined effects of high oil price and low agricultural product price may provide an opportunity to utilize biomass to replace petroleum oil as raw materials for the chemical industry (*1*).

As is well-known, cellulose occurs mostly as lignocellulose in complex association with lignin and hemicellulose, a polymer composed of anhydroglucose monomer units, which forms a macromolecule with a highly stable crystalline lattice structure. Thereby, cellulose is strongly resistant to attack both by enzymes and by chemical agents, such as acidic compounds (*2*,*3*). To date, the different techniques are available for the conversion of the cellulose into fermentable sugars. Some of them are based on acid hydrolysis utilizing either dilute or concentrated acids, such as sulphuric acid or hydrochloric acid, while other techniques are based on a pretreatment of the raw material, such as steam explosion, followed by an enzymatic hydrolysis (*4*,*5*). At present, the efficiency of enzyme is limited; the actual yield of the enzyme saccharification rarely surpasses chemical hydrolysis. The enzymatic process is dependent on the effectiveness of the pretreatment and requires additional substrate because it has to be produced from cellulosic biomass. Furthermore, the enzymatic process also is a slow process (*6*−*8*). Thereby, it is not likely to be applied in industrial practice in the immediate future. Although acid hydrolysis has some faults, it still is one of the viable methods currently being developed as a promising means of producing sugar from cellulose.

Formic acid with hydrochloric acid as the catalyst has been shown to effectively dissolve cellulose (*2*). After hydrolysis during dissolution, solid hydrolysates of soluble sugar oligomers can be obtained. Monomeric glucose sugars comprise a significant proportion of the resultant hydrolysates (*9*). The hydrolysis of cellulose in formic acid with hydrochloric acid is a reaction system in which formic acid itself acts as a catalyst. Formic acid, together with hydrochloric acid, can be effectively recovered and reused (*2*, *3*). In this study, the formic acid system was established for hydrolysis of cellulosic fiber from bamboo pulp to produce fermentable sugars for further conversion to bioenergy, ethanol or butanol.

MATERIALS AND METHODS

The Hydrolysis of Cellulose. Bamboo sulfite pulp, used as materials of cellulosic fiber with 97.5% of content of cellulose, was provided by the jiangmen Sugar Cane Chemical Factory (Group) Co., Ltd. (China). Formic acid was purchased from the Shanghai Lingfeng (China), and hydrochloric acid was purchased from the Guangdong Donghong Chemical Company (China).

Four grams of bamboo pulp was placed in a three-neck flash with stirrer device containing 96 g of formic acid solution (78.22% formic acid and 17.78% water) with additional hydrochloric acid at a ratio of 4% (w/w). The reaction was carried out at different temperatures and residence times. After the reaction, formic acid and hydrochloric acid were extracted by vacuum distillation. The degradation products of sugars extracted by ethanol and analyzed by GC−MS. The final remains were retained for further analysis after washing and freezing desiccation.

*Corresponding author. Tel: 86-020-22236719. Fax: 86-020-22236719. E-mail: lclulin@scut.edu.cn.

© 2010 American Chemical Society

Published on Web 01/29/2010

The yield of glucose (Y_G%) and reduced sugar (Y_S%) were calculated by equations as follows:

$$Y_G\% = \frac{m_G}{m_C} \times 100\%$$

$$Y_S\% = \frac{m_S}{m_C} \times 100\%$$

m_G is the mass of glucose, m_S is the mass of reduced sugars, m_C is the mass of cellulose.

High Performance Liquid Chromatography (HPLC) Analysis. The HPLC system consisted of a system controller (Waters 600E, Milford, MA), an automatic sampler (Waters 717), a differential refractometer (Waters 410), and a Sugar-Pak I column (Waters). The mobile phase was distilled water and was run at a flow rate of 1.1 mL min^{-1}. The LC system was operated at 90 °C. The sample volumes injected were 10 μL. Standard samples and hydrolysate samples were filtered before analysis using a 0.22 μm filter.

^{13}C Solid-State Nuclear Magnetic Resonance (NMR). Cross-polarization/magic angle spinning (CP/MAS) ^{13}C solid-state NMR experiments were performed on a Bruker Avance 400 spectrometer (Bruker BioSpin, Karlsruhe, Germany) operating at a frequency of 100.61 MHz with a 4 mm MAS BB-1H probe at 25 °C. The contact time for CP was 1.5 ms with a proton 90° pulse of 5.6 μs. The MAS speed was 5 kHz. The delay time after the acquisition of the free induction decay signal was 3s.

The crystallinity (Cr.I.) and amorphicity (Am.I.) indices, given as a percentage of the integrals of the C_4 peaks at 86−92 (*a*) and 80−86 ppm (*b*), were calculated by the following equations (*10*, *11*):

$$\text{Cr.I. } (\%) = 100a/(a+b)$$
$$\text{Am.I. } (\%) = 100 - \text{Cr.I.}$$

X-ray Diffraction Analysis. Wide-angle X-ray diffraction was conducted using a D/MAX-III (Rigaku, Tokyo, Japan), with 12° min^{-1} scan speed. Cellulose powder samples were laid on the glass sample holders (35 × 50 × 5 mm) and analyzed under plateau conditions. Copper radiation was generated at a voltage of 40 kV and a current of 30 mA. The scan scope was between 2 and 50°.

The degree of crystallinity (χ_c) was calculated by (*11*, *12*)

$$\chi_c = F_c/(F_a + F_c) \times 100\%$$

where F_c and F_a are the areas of the crystal and noncrystalline regions, respectively.

The relative crystallite size was calculated from the Scherrer equation, using the method based on the width of the diffraction patterns. The relative crystallite sizes were determined from the 101, 002, and 021 lattice planes of the cellulose samples:

$$D_{hkl} = \frac{K\lambda}{\beta_0 \cos\theta}$$

where D_{hkl} is the size of the crystallite (nm), K is the Scherrer constant (0.94), λ is X-ray wavelength, if a copper target was used, and the λ is 0.15418 nm. β_0 is the full-width at half-maximum of the reflection *hkl*; measured in 2θ is the corresponding Bragg angle (*13*).

GC−MS analysis. The degradation products of glucose have been analyzed by Agilent 5975 inert gas chromatograph−mass spectroscopy.

The chromatographic column is a capillary column wax 30 m × 0.25 mm × 1.5 μm. The carrier gas is helium with flow control mode as pressure. The pressure is at 34.0 kPa, and total flow is at 84.3 mL/min. Column flow is 0.80 mL/min with a linear velocity of 32.4 m/s. The purge flow is 3.0 mL/min with a split ratio of 40. The temperature of column is held at 40 °C for 3 min before increasing at a heating rate of 5 °C/min. When the desired column temperature of 250 °C is reached, it is held for 10 min.

Mass spectroscopy is based on EI. The ion source temperature is at 200 °C, and the electric energy is 70 eV. The emission electricity is 60 μA, while the interface temperature is at 300 °C. The detector gain is set at 0.7 kV with a threshold of 1000. The acquired mode is scan with an interval of 0.5 s, scan speed of 3333 and scan range of *m*/*z* 30−500.

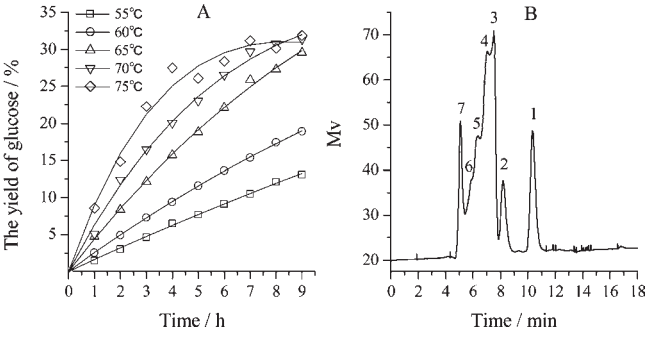

Figure 1. Effect of residence time and temperature on the release of glucose by bamboo fiber (**A**) and representative HPLC chromatogram of hydrolysates of bamboo fibers (**B**) during the hydrolysis in formic acid solution (formic acid to water weight ratio of 0.782:0.178) with 4% hydrochloric acid). 1, glucose; 2, cellobiose; 3, cellotriose; 4, cellotetrose; 5, cellopentose; 6, cellohexose; 7, residual formic acid.

Table 1. The Yield of Reducing Sugars from Hydrolysate of Bamboo Fiber Obtained through the DSN Method

	yield of reducing sugars (%)				
time (h)	55 °C	60 °C	65 °C	70 °C	75 °C
1	7.30	9.15	11.60	20.91	24.42
2	11.06	12.12	20.20	24.98	27.99
3	13.74	17.19	30.52	24.88	28.91
4	15.57	21.82	30.90	36.78	29.03
5	16.55	27.71	31.54	36.85	29.60
6	22.90	28.14	32.78	37.51	30.68
7	23.60	30.58	31.09	30.86	31.44
8	24.83	30.84	31.36	28.58	33.21
9	23.15	31.90	31.81	24.42	32.08

RESULTS AND DISCUSSION

Effect of Temperature and Residence Time on the Hydrolysis of Bamboo Fibers. During the hydrolysis of bamboo fiber in the formic acid system, the reaction temperature (55 °C, 60 °C, 65 °C, 70 °C and 75 °C) and residence time (from 0 to 9 h, interval 30 min) was investigated. The results are shown in **Figure 1A**. The yield of glucose increased with the prolongation of time at 55 °C, 60 °C, 65 °C and 70 °C, with the yield of 13.1%, 18.9%, 29.6%, 31.4% and 31.9% at 9 h respectively. Before 7 h, the yield of glucose increased with the prolongation of time at 75 °C and then leveled off. The yield of glucose increased rapidly before 3.5 h, and then the rate slowed. After 7 h, the yield reached a maximum at 31.9%, then decreased. Temperature had a dramatic effect on the hydrolysis of bamboo fiber, the yield of glucose at 65 °C was more than twice of that at 55 °C, and the yield of glucose at 75 °C was about two times of that at 65 °C before 5 h, after which they became the same. The glucose degradation in mineral acid solution has been reported in numerous papers (*14*−*16*). These results suggest that high temperature accelerated the rate of hydrolysis, but also accelerated the degradation during the hydrolysis in formic acid solution (formic acid to water weight ratio of 0.782:0.178) with 4% hydrochloric acid. Finally, the yield of glucose increased little after 3.5 h at 75 °C. The percentage of glucose in the water-soluble sugar/sugar oligomers mixture gradually increased. Water-soluble sugar mixtures were analyzed by HPLC. Glucose, cellubiose, cellotriose, cellotetrose, cellopentose and cellohexose have been detected in the hydrolysates (**Figure 1B**).

The yield of reducing sugars measured by the DSN method is shown in **Table 1**. The yield of reducing sugars first increased

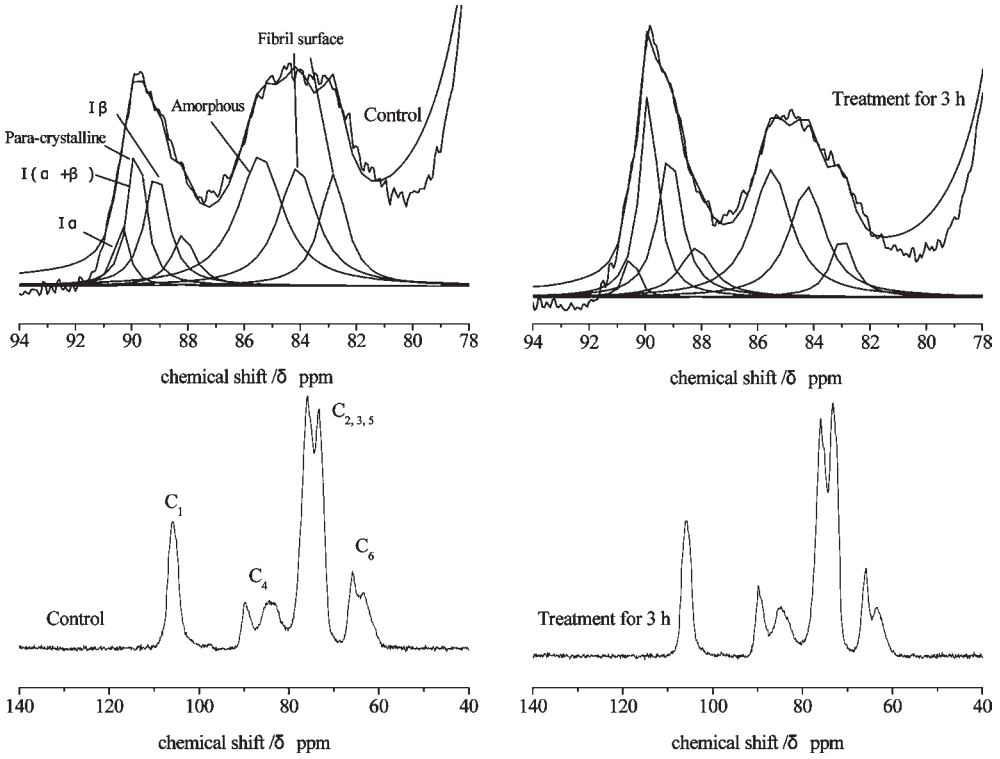

Figure 2. CP/MAS ^{13}C NMR spectra and fitting of the C_4 region of spectrum from bamboo fiber. The chemical shift, relative intensity and type of the individual lines are shown in **Tables 2** and **3**.

Table 2. Peak Assignment (ppm) Values in ^{13}C NMR Spectra of Bamboo Fiber

control				treatment for 3 h			
C_1	C_4	$C_{2,3,5}$	C_6	C_1	C_4	$C_{2,3,5}$	C_6
105.853	84.375	75.917	65.844	106.005	89.825	75.948	65.917
	89.682	73.308	63.419		84.807	73.196	63.524

rapidly and then leveled off or decreased little with the extension of residence time. The enhancement was more pronounced over 60 °C. Therefore, at high temperatures the reducing sugars were severely degraded, which was consistent with the degradation of glucose in formic acid with hydrochloric acid.

Structure Changes of Bamboo Fibers during Hydrolysis in the Formic Acid Reaction System. The CP/MAS ^{13}C solid-state NMR spectra of bamboo fiber for detection of changes of its structure are shown in **Figure 2**. The resonance signals of the samples after being treated for 3 h were similar to those of the control. The main ^{13}C peak assignment values are shown in **Table 2**. The peak assignments of C_1, C_4, and C_6 were confirmed by site-specific labeling with ^{13}C and biosynthesis, but the $C_{2,3,5}$ peaks assignment could not be assigned (*17*−*20*). Teeäär and Lippmaa (*21*) tried to indirectly assign the $C_{2,3,5}$ regions of the CP/MAS ^{13}C NMR spectrum of cotton cellulose (I_β-rich cellulose), based on consideration of the ^{13}C spin−lattice relaxation times. They assigned the low-field doublet at 76.8 ppm and 76.0 ppm to C_2 as the closest neighbor to the C_1 doublet. They also assigned the singlet line at 73.0 ppm to C_5, and the remaining line at 74.2 ppm to C_3, because the 74.2 ppm relaxed faster than the other lines in the cluster region. However, Kono et al. (*17*) assigned the doublet line at 76.8 ppm and 76.0 ppm to C_3 by using ^{13}C-labeled cellulose biosynthesized from D-[1,3-^{13}C] glycerol. This interpretation was also supported by experiments using ^{13}C-labeled cellulose from D-[2-^{13}C]glucose, and it was shown that the resonance lines for C_5 were split into a doublet in both subspectra of the I_α and I_β phases. For the assignment of the ^{13}C signal of cellulose in the solid state, Bardet et al. (*22*)applied the two-dimensional spin-exchange solid-state NMR technique to ^{13}C-enriched wood chips from aspen (*Populus euramericana*) grown under a 20% $^{13}CO_2$ atmosphere, and observed two broad signals around 76 and 74 ppm, in the region of the signals corresponding to C_2, C_3, and C_5. They assigned the signal around 76 ppm to C_2, and that at 74 ppm to C_3 and C_5, by comparing the intensities of the signals as a function of increasing mixing time.

Though the solid-state structure differed widely between the samples, the most pronounced tendency through the series is the deterioration of spectral details from highly ordered to less-ordered cellulose. This is most clearly visible in the C_4 (δ 80−91 ppm) regions of the spectra. The cellulose signal clusters were decomposed into contributing lines by a nonlinear least-squares fitting of NMR spectra (Lorentzian fit), based on the quantification of the CP/MAS ^{13}C NMR spectra. The results of the nonlinear least-squares fitting of the C_4 regions of the bamboo fiber are shown in **Figure 2**. The assignments and relative intensities are given in **Table 3** (*23*).

The most informative region in the NMR spectrum of cellulose is the signal cluster with a chemical shift distribution between δ 80−92 ppm. The fairly sharp signals from δ 86−92 ppm corresponded to C_4 carbons from crystalline forms together with para-crystalline domains, whereas the broader upfield resonance line from δ 80−86 ppm is assigned to the amorphous domains (*23*, *24*). Wickholm et al. (*25*) and Larsson et al. (*24*) thought that the region typical of the less ordered carbohydrate forms (80−86 ppm) contains several signals from the amorphous region and the accessible surface of the cellulose; the 86−91 ppm signals come from the crystalline region, the "in-core" fiber, and the inaccessible surfaces of the cellulose.

Despite the apparent multiplicity of signals arising from the disordered regions, it is nevertheless possible to evaluate an "apparent crystallinity index" by integrating all the contributions

Table 3. Assignments and Intensity of a Nonlinear Least-Squares Fitting of the C_4 Region of the CP/MAS ^{13}C NMR Spectra of Bamboo Fiber

	control			treatment for 3 h		
assignment	chemical shift (ppm)	intensity/%	Cr.I./%	chemical shift (ppm)	intensity/%	Cr.I./%
Iα	90.36	4.23		90.48	2.68	
I (α + β)	89.81	11.52		89.87	18.54	
para-crystalline	89.12	12.89		89.12	17.33	
Iβ	88.17	5.74	30.54	88.19	8.22	40.22
amorphous	85.42	29.17		85.50	25.82	
fibril surface	84.09	22.17		84.23	20.62	
fibril surface	82.83	14.28		82.99	6.78	

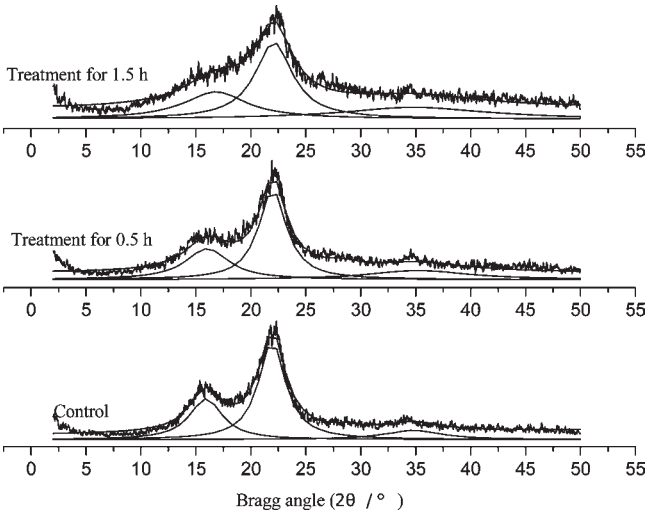

Figure 3. The X-ray diffraction profiles of bamboo fiber.

arising from the disordered regions, i.e. surface chains, crystal defects, and amorphous material, including hemicelluloses, into the amorphous part of the cellulose (*10*, *11*). As seen in **Table 3**, the crystallinity index of bamboo fiber is 30.54%, which increases 9.68% after treatment for three hours. The bamboo fiber contained partly amorphous hemicellulose and lignin, which could be dissolved and hydrolyzed during the hydrolysis. At the same time, the acid also could penetrate into the inner part of the cellulose, the bamboo fiber was hydrolyzed and the structure of the cellulose was broken. The power of bamboo fiber became smaller, thereby the bamboo fiber bundled together to decrease the surface energy, and the surface area decreased. The acid solution initially acted on the surface, and then simultaneously affected the amorphous and crystalline zones of the fibers, until the rigid crystalline lattice framework of the cellulose was crushed. The amorphous zone is more easily hydrolyzed than the crystalline zone and the surface area decreased, thereby the crystallinity index of NMR increased.

Figure 3 shows the X-ray diffraction profiles of the bamboo fibers. The representative peaks are observed at $2\theta = 14.7°$, 16.3° for the (101) plane; $2\theta = 22.5°$ for the (002) plane; and $2\theta = 34.5°$ for the (004) plane. In these diffraction profiles, the peaks at $2\theta = 22.5°$ of the control cellulose sample are higher and sharper than those after formic acid treatments for 30 and 90 min. The diffraction intensity of the shoulder of the peak around $2\theta = 20°$ decreases to a noticeable extent. The separation between peaks at $2\theta = 14.7°$ and 16.3° in the treated samples is ambiguous, but considerably clearer than in the control sample. One can conclude that the crystalline intensity of bamboo fiber is reduced gradually, which is especially evident on the 101 and the 002 lattice planes (**Figure 3**).

Table 4 shows the relative crystalline degree as calculated from X-ray diffraction data of bamboo fibers. The relative crystalline

Table 4. Characteristic X-ray Diffraction Peaks and Degree of Crystallinity of Bamboo Fibers

lattice plane	Bragg angle 2θ/deg	intensity/cps	crystalline size/nm	crystallinity degree/%
		Control		
101	15.913	443	2.32	
002	21.930	862	2.88	58.30
040	34.766	205	1.34	
		Treatment for 0.5 h		
101	16.024	338	1.73	
002	21.985	742	2.79	52.22
040	35.264	177	0.78	
		Treatment for 1.5 h		
101	16.797	283	1.21	
002	22.091	646	2.06	46.27
040	34.879	196	0.57	

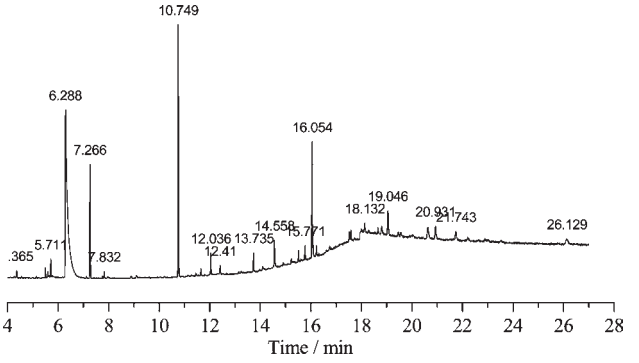

Figure 4. GC spectrum of bamboo fiber hydrolysis products in formic acid solution with 4% hydrochloric acid.

degree decreased from 58.30% to 52.22% after the sample had been treated for 30 min. 90 min later the relative crystalline index declined further to 46.27%. The relative crystalline size also declined with the reaction time. As the X-ray diffraction relative crystalline index and crystalline size dropped gradually, the cellulose was also dissolved in a stepwise fashion in formic acid. Therefore, the effect of formic acid on the crystalline zone was more distinctive than that on the amorphous zone. As a result, the crystalline lattice of cellulose was strongly burst, and eventually the rigid framework of crystalline lattice of cellulose was crushed.

Degradative Side Reaction of Glucose and Reducing Sugars during the Hydrolysis of Bamboo Fiber. The hydrolysis of cellulose is strongly dependent on the temperature. High temperature can enhance the transformation ratio of cellulose to glucose. However, degradative side reaction of glucose could take place and speed up with the increase of temperature (*1*−*3*, *16*, *26*), and

Table 5. Hydrolysis Products of Bamboo Fiber at the Influence of Aluminum Iso-propoxide and Acetone in Formic Acid Solution with 4% Hydrochloric Acid

			contents (%)		
no.	main compounds	time (min)	control	with aluminum iso-propoxide	with acetone
1	acetic acid	5.572		2.14	0.69
2	furfural	5.730	1.52	2.98	2.51
3	formic acid	6.285	46.82	73.64	15.55
4	ethyl levulinate	7.264	10.47	5.53	38.14
5	5-methyl-2(5*H*)-furanone	8.168			0.16
6	5-[(formyloxy)methyl]-2-furancarboxaldehyde	10.742	16.72	6.28	13.87
7	methyl-2-furoate	11.650	0.61		1.10
8	5-hydroxymethyl furfural	16.050	14.01	9.44	23.94
9	1,4-anhydro-D-mannitol	19.056	9.84		

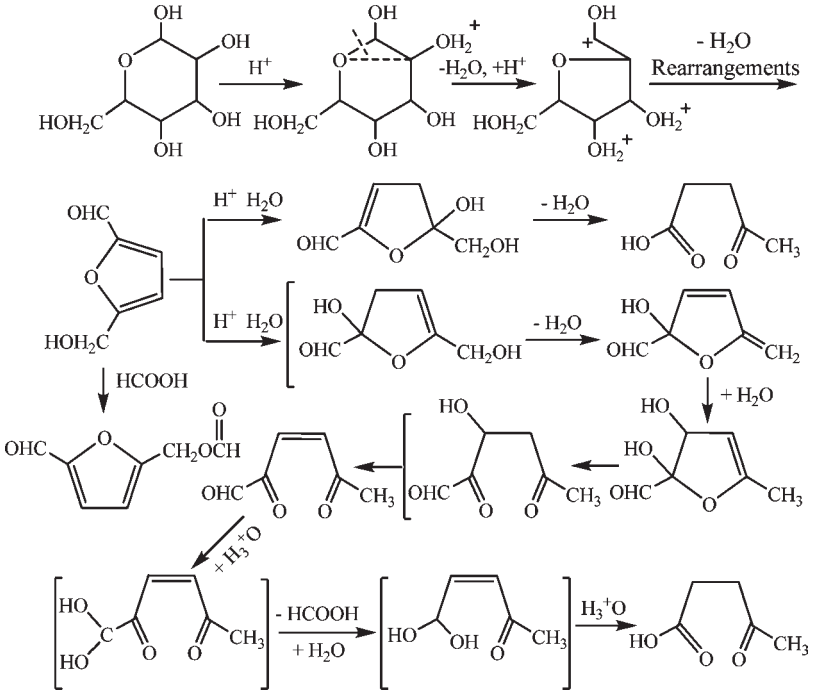

Figure 5. The possible reaction pathway for β-D-glucose degradation initiated at the 2-OH surrounded by acid.

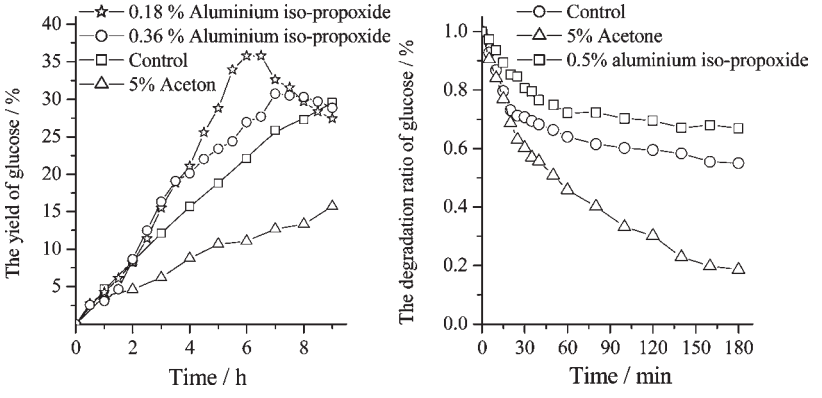

Figure 6. The influence of aluminum iso-propoxide and acetone on the hydrolysis of bamboo fiber and degradation of glucose with residence time and temperature in formic acid solution with 4% hydrochloric acid.

exploration of pathway of degradation of glucose and reducing sugars will play an important role in preventing extensive loss of fermentable sugars.

During the hydrolysis of bamboo fiber, the glucose and reducing sugars also were degraded. The ring of β-D-glucose has five hydroxyl groups. It is not difficult to imagine that the degradation pathway is very complex. In order to reveal the cause of β-D-glucose degradation in formic acid solutions, the degradation products were analyzed using GC−MS. The results are shown in **Figure 4**. The main degradation products are shown

in **Table 5**. The hydroxyl group on the 2-carbon is easily protonated, followed by those on the third and fourth carbons. The hydroxyl groups on the first and the sixth are relatively stable (*27*). The hydroxyl groups on the ring of β-D-glucose are exposed to the hydronium ions. Therefore, they are easily protonated and cleaved off and the carbon cations are formed. Still, the carbon cations can rearrange, and thus various compounds are formed as a result. The main degradation products in formic acid with hydrochloric acid are found to be ethyl levulinate, 5-hydroxymethyl furfural, 5-[(formyloxy)methyl]-2-furancarboxaldehyde and 1,4-anhydro-D-mannitol. The formic acid is the residue of solvent and reaction production. The ethyl levulinate is generated from levulinic acid reaction with ethanol, which is the extraction reagent. This is a dehydration reaction. However, levulinate acid comes from 5-hydroxymethyl furfural through dehydration and rearrangements (*1*, *28*, *29*). 5-[(Formyloxy)methyl]-2-furancarboxaldehyde may come from the esterification reaction between 5-hydroxymethyl furfural with formic acid. 1,4-*anhydro*-D-Mannitol possibly comes from the dehydration reaction and rearrangements of hydroxyl on the ring of glucose. Therefore, the main degradation product of β-D-glucose is 5-hydroxymethyl furfural. There are two degradation pathways of 5-hydroxymethyl furfural to levulinic acid: one is addition reaction with water on the double bond of the second and third carbons, and the other is addition reaction with water on the double bond of the fourth and fifth carbons. Through deduction, the main degradation pathway of glucose is that the hydroxyl group on the 2-carbon is protonated and cleaved off. **Figure 5** is a sketch of the deduced degradation pathway.

One effective method to increase the yield of glucose is to prevent the degradation of glucose. When the 0.5% aluminum iso-propoxide was added into the reaction system, the yield of glucose increased 10−20%, and aluminum iso-propoxide reduced the rate of degradation of glucose. But 5% acetone reduced the yield of glucose more than 50%. Acetone cannot catalyze the hydrolysis of cellulose; in some diluted acid hydrolysis, acetone can reduce the degradation of glucose, but in the formic acid system, 5% acetone accelerated the degradation of glucose quickly. In order to reveal the influence of aluminum iso-propoxide and acetone on the degradation of glucose, the compounds were analyzed by GC−MS. The results are shown in **Table 5**. The main compounds are ethyl levulinate (L), 5-[(formyloxy)methyl]-2-furancarboxaldehyde (FE), 5-hydroxymethyl furfural (F), and 1,4-*anhydro*-D-mannitol (M). The ratios of compounds L:FE:F is 1:1.60:1.34 in the control reaction solution, 1:1.14:1.71 in the reaction solution with 0.5% aluminum iso-propoxide and 1:0.36:0.63 in the reaction solution with 5% acetone. The results indicated that aluminum iso-propoxide prevented the production of 5-[(formyloxy)methyl]-2-furancarboxaldehyde, and acetone catalyzed the production of levulinic acid and prevented the production of 5-[(formyloxy)methyl]-2-furancarboxaldehyde. Both aluminum iso-propoxide and acetone prevented the production of 1,4-*anhydro*-D-mannitol. **Figure 6** also indicated that aluminum iso-propoxide prevented the degradation of glucose and acetone promoted the degradation of glucose to levulinic acid.

LITERATURE CITED

(1) Fang, Q.; Hanna, M. A. Experimental studies for levulinic acid production from whole kernel grain sorghum. *Bioresour. Technol.* **2002**, *81* (3), 187–192.

(2) Sun, Y.; Lin, L.; Pang, C. S.; Deng, H. B.; Peng, H.; Li, J. Z.; He, B. H.; Liu, S. J. Hydrolysis of cotton fiber cellulose in formic acid. *Energy Fuels* **2007**, *21* (4), 2386–2389.

(3) Sun, Y.; Zhuang, J. P.; Lin, L.; Ouyang, P. Clean conversion of cellulose into fermentable glucose. *Biotechnol. Adv.* **2009**, *27* (5), 625–632.

(4) Sun, Y.; Cheng, J. J. Dilute acid pretreatment of rye straw and bermudagrass for ethanol production. *Bioresour. Technol.* **2005**, *96* (14), 1599–1606.

(5) Orozco, A.; Ahmad, M.; Rooney, D.; Walker, G. Dilute Acid Hydrolysis of Cellulose and Cellulosic Bio-Waste Using a Microwave Reactor System. *Process Saf. Environ. Prot.* **2007**, *85* (5), 446–449.

(6) Sivers, M.; Zacchi, G. A techno-economical comparison of three processes for the production of ethanol from pine. *Bioresour. Technol.* **1995**, *51* (1), 43–52.

(7) Solomon, B. D.; Barnes, J. R.; Halvorsen, K. E. Grain and cellulosic ethanol: History, economics, and energy policy. *Biomass Bioenergy* **2007**, *31* (6), 416–425.

(8) Lee, Y. Y.; Iyer, P.; Torget, R. W. Dilute-Acid Hydrolysis of Lignocellulosic Biomass. *Adv. Biochem. Eng./Biotechnol.* **1999**, *65*, 93–115.

(9) Kamm, B.; Kamm, M.; Schmidt, M.; Starke, I.; Kleinpeter, E. Chemical and biochemical generation of carbohydrates from lignocellulose feedstock (Lupinus nootkatensis)-quantification of glucose. *Chemosphere* **2006**, *62*, 97–105.

(10) Heux, L.; Dinand, E.; Vignon, M. R. Structural aspects in ultrathin cellulose microfibrils followed by ^{13}C CP-MAS NMR. *Carbohydr. Polym.* **1999**, *40* (2), 115–124.

(11) Focher, B.; Palma, M.; Canetti, T.; Torri, M.; Cosentino, G. C.; Gastaldi, G. Structural differences between non-wood plant celluloses: evidence from solid state NMR, vibrational spectro scopy and X-ray diffractometry. *Ind. Crops Prod.* **2001**, *13* (3), 193–208.

(12) Zhou, D.; Zhang, L.; Guo, S. Mechanisms of lead biosorption on cellulose/chitin beads. *Water Res.* **2005**, *39* (16), 3755–3762.

(13) Oh, S. Y.; Yoo, D. I.; Shin, Y.; Kim, H. C.; Kim, H. Y.; Chung, Y. S.; Park, W. H.; Youk, J. H. Crystalline structure analysis of cellulose treated with sodium hydroxide and carbon dioxide by means of X-ray diffraction and FTIR spectroscopy. *Carbohydr. Res.* **2005**, *340* (15), 2376–2391.

(14) Johansson, L.; Virkki, L.; Anttil, H.; Esselstrom, H.; Tuomainen, P.; Sontag-Strohm, T. Hydrolysis of β-glucan. *Food Chem.* **2006**, *97*, 71–79.

(15) Lloyd, T. A.; Wyman, C. E. Combined sugar yields for dilute sulfuric acid pretreatment of corn stover followed by enzymatic hydrolysis of the remaining solids. *Bioresour. Technol.* **2005**, *96*, 1967–1977.

(16) Mosier, N. S.; Ladisch, C. M.; Ladisch, M. R. Characterization of acid catalytic domains for cellulose hydrolysis and glucose degradation. *Biotechnol. Bioeng.* **2002**, *79*, 610–618.

(17) Kono, H.; Yunoki, S.; Shikano, T.; Fujiwara, M.; Erata, T.; Takai, M. CP/MAS ^{13}C NMR Study of Cellulose and Cellulose Derivatives. 1. Complete Assignment of the CP/MAS ^{13}C NMR Spectrum of the Native Cellulose. *J. Am. Chem. Soc.* **2002**, *124* (25), 7506–7511.

(18) Kono, H.; Erata, T.; Takai, M. Complete Assignment of the CP/MAS ^{13}C NMR Spectrum of Cellulose III_I. *Macromolecules* **2003**, *36* (10), 3589–3592.

(19) Kono, H.; Numata, Y. Two-dimensional spin-exchange solid-state NMR study of the crystal structure of cellulose II. *Polymer* **2004**, *45* (13), 4541–4547.

(20) Witter, R.; Sternberg, U.; Hesse, S.; Kondo, T.; Koch, F.-T.; Ulrich, A. S. ^{13}C Chemical Shift Constrained Crystal Structure Refinement of Cellulose I_α and Its Verification by NMR Anisotropy Experiments. *Macromolecules* **2006**, *39* (18), 6125–6132.

(21) Teeäär, R.; Lippmaa, E. Solid state carbon-13 NMR of cellulose. A relaxation study. *Polym. Bull.* **1984**, *12* (4), 315–18.

(22) Bardet, M.; Emsley, L.; Vincendon, M. Two-dimensional spin-exchange solid-state NMR studies of ^{13}C-enriched wood. *Solid State Nucl. Magn. Reson.* **1997**, *8* (1), 25–32.

(23) Larsson, P. T.; Wickholm, K.; Iversen, T. A. CP/MAS^{13}C NMR investigation of molecular ordering in celluloses. *Carbohydr. Res.* **1997**, *302* (1−2), 19–25.
(24) Larsson, P. T.; Hult, E. L.; Wickholm, K.; Pettersson, E.; Iversen, T. CP/MAS ^{13}C-NMR spectroscopy applied to structure and interaction studies on cellulose I. *Solid State Nucl. Magn. Reson.* **1999**, *15* (1), 31–40.
(25) Wickholm, K.; Larsson, P. T.; Iversen, T. Assignment of non-crystalline forms in cellulose I by CP/MAS ^{13}C NMR spectroscopy. *Carbohydr. Res.* **1998**, *312* (3), 123–129.
(26) Cha, J. Y.; Hanna, M. A. Levulinic acid production based on extrusion and pressurized batch reaction. *Ind. Crops Prod.* **2002**, *16* (2), 109–118.
(27) Qian, X.; Nimlos, M. R.; Davis, M. Ab initio molecular dynamics simulations of β-D-glucose and β-D-xylose degradation mechanisms in acidic aqueous solution. *Carbohydr. Res.* **2005**, *340*, 2319–2327.
(28) Cha, J. Y.; Hanna, M. A. Levulinic acid production based on extrusion and pressurized batch reaction. *Ind. Crops Prod.* **2002**, *16* (2), 109–118.
(29) Horvat, J.; Klaić, B.; Metelko, B.; Šunjić, V. Mechanism of levulinic acid formation. *Tetrahedron Lett.* **1985**, *26* (17), 2111–2114.

Received for review November 8, 2009. Revised manuscript received January 14, 2010. Accepted January 14, 2010. The authors are grateful for the financial support from the National Key Basic Research Program (2010CB732201) from the Ministry of Science and Technology of China, the Natural Science Foundation of China (50776035, U0733001), the Foundation of Scientific Research for Universities (20070561038), the Initiative Group Research Project (IRT0552) from the Ministry of Education of China, the National High Technology Project (Project 863) (2007AA05Z408), the Science Foundation for Post Doctorate Research from the Ministry of Science and Technology of China (20090450863), National Key Basic Research Program (2010CB-732201) and the National Key R&D Program (2007BAD34B01) 453 from the Ministry of Science and Technology of China.